Knot detection in coarse resolution CT images of logs

Julie COOL[a], Magnus FREDRIKSSON[b], Stavros Avramidis[a]

[a] Department of Wood Science, Faculty of Forestry, University of British Columbia
Forest Sciences Centre, 2424 Main Mall, Vancouver BC Canada V6T 1Z4
[b] Division of Wood Science and Technology, Luleå University of Technology, SE-931 87 Skellefteå, Sweden

ABSTRACT

The use of X-ray computed tomography (CT) scanning of logs in sawmill has become a reality in the last few years, usually with rather costly and complex machines resembling medical scanners. However, a scanning solution has been developed that is less costly and more robust, and therefore more suited for sawmill needs. The rather coarse data from this machine has not been fully evaluated regarding possibilities to detect internal features such as knots. In this study, a knot detection algorithm developed for medical-type scanners was applied to images of four different logs of various species obtained from a coarse resolution scanner. The objective was to see if it was possible to detect knots automatically in the images. If so, the aim was to calculate the knot detection rate and the accuracy of detected knot size and position. These numbers were calculated compared to manually measured reference knots. This resulted in a knot detection rate of about 67 % overall, a well detected knot position, but poorly detected knot size. The material was too small to draw any definite conclusions, but as a preliminary study it provides input for further investigation on knot detection in coarse resolution X-ray CT images. Future work involves scanning more logs to get more data, and to pinpoint the resolution needed for accurate knot detection using the current algorithm.

Keywords: X-ray CT Scanning, Image resolution, Knot detection

INTRODUCTION

X-ray computed tomography (CT) scanning for industrial use in the wood industry is becoming a reality in sawmills, for instance the scanner presented by Guidiceandrea, Ursella, and Vicario (2011). This technology is based on medical applications, and produces images of rather high resolution, but at a large cost. In addition, the size limit on the objects that can be scanned in such systems is usually rather small.

However, other alternatives are being developed, such as the cone-beam scanner described by An and Schajer (2014a, 2014b). They utilize *a priori* knowledge of log geometry to simplify both the scanning and subsequent reconstruction process. In addition, the log is rotated instead of the scanner gantry, which removes the need for complicated technical solutions for power supply and information transfer to and from a device rotating at high speed.

To utilize such a scanner in a sawmill application it would be necessary to find internal features of logs in the CT data that can then be used to control the sawing process. One of the most important features when it comes to board quality is knots, since they affect both visual appearance as well as strength and stiffness. Therefore, it is of interest to be able to detect knots in CT data. Since frequency, size and position of knots have a large impact on board quality, these quantities need to be evaluated if detected knots were to be used for process control in sawmills.

The objective was to apply the knot detection algorithm from Johansson et al. (2013) to reconstructed CT data from the coarse resolution cone-beam scanner developed by An and Schajer (2014a, 2014b), and to compare the results of knot detection to manual reference measurements. By doing this, it was possible to assess whether or not the resolution of these X-ray images is high enough to find knots. In addition, a comparison to previous research on high-resolution CT data was done.

MATERIALS AND METHODS

Sampling of logs

Four logs were used in this study, one western redcedar (*Thuja plicata* Donn ex D. Don) log, one white spruce (*Picea Glauca* (Moench) Voss) log and two Douglas-fir (*Pseudotsuga menziesii* (Mirb.) Franco) logs. They were sampled from a log yard in British Columbia, Canada, so there is no detailed information available regarding the origin of the logs. They were cut into rather short lengths of 0.5 to 1.2 meters.

Scanning

The logs were scanned using the lab-built scanner described in An and Schajer (2014a). The working principle is that an object is illuminated by an industrial cone-beam X-ray source, the X-rays being detected by a two dimensional matrix of X-ray detectors. During sampling, the object is rotated in order to make measurements from different angles. The distance from the X-ray source to the detector was in this case 1.1 m, with the center of the field of view located 0.52 m from the source. The detector size was 0.41 × 0.41 m. The scans were done using a voltage of 140 kVp and a 5 mA current.

Reconstruction

The sampled X-ray data was used for reconstruction of log density images using the method described by An and Schajer (2014b). This resulted in stacks of CT images. The data was separated in two sets, with two logs in each. A slightly different resolution was used in the two data sets, which are summarized in Table 1. The log top diameter was measured using the detected log outer shape, using a simple thresholding operation on the CT stacks. A bit depth of 8 was used for all images, and the image size was 146 × 146 pixels in each cross-section. Figure 1 shows four example cross-section images, one from each log.

Table 1: Properties of the two data sets and the four logs.

Data set number	1		2	
Voxel dimension (mm)	1.446 × 1.446 × 4		1.430 × 1.430 × 4	
Log wood species	white spruce	Douglas-fir 1	western redcedar	Douglas-fir 2
Log length (cm)	120	73	88	53
Log top diameter (cm)	14	14	15	14

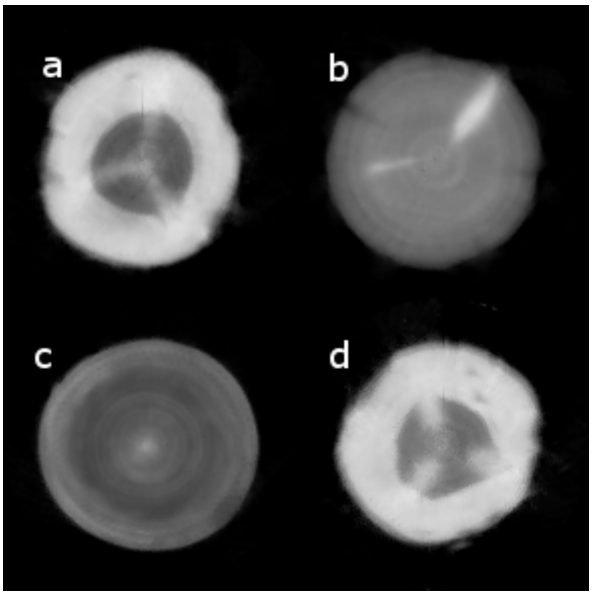

Figure 1: Four examples of cross-section CT images where a) is the Douglas-fir log of data set 1, b) is the white spruce log of data set 1, c) is the western redcedar log of data set 2, and d) is the Douglas-fir log of data set 2.

Knot detection algorithm

The knot detection algorithm developed by Johansson et al. (2013) was applied to the CT stacks. Prerequisites for the algorithm are a detected pith position, an outer shape border and a sapwood-heartwood border. Pith detection was done by using Hough transforms as described by Longuetaud et al. (2004). Sapwood–heartwood and outer shape border were found using a series of filters applied on polar images of the logs' CT images, where the polar images had

their origin at the pith. This was basically the algorithm described by Longuetaud, Mothe and Leban (2007), with the modifications described by Baumgartner, Brüchert and Sautner (2010). Both borders were described by polar coordinates for each CT cross-section, with 360 points for each slice, i.e. one radius at every angular degree.

In short, the knot detection algorithm works by creating concentric surfaces (CS's) that extend outwards from the pith of the log. The CS's are close to cylindrical shells cut out at a certain radius in the CT stacks, following either the heartwood shape or the outer shape of the log. This creates veneer-like structures, showing knots as oval or round shapes. Ten CS's are used for each log, of which at least five need to be from the heartwood since knots are more easily found in the heartwood (Pietikäinen 1996, Tong et al. 2013). In all heartwood CS's, knot objects are found using a thresholding operation, after which ellipses are fit to the objects if these are of a reasonable size and orientation. The knot ellipses are then matched together to form knots. The knots in the heartwood are then extrapolated to trace knots in the sapwood, by finding regions of interest in the sapwood CS's and using morphological dilation to find the position and size of the knot within that region. After this, the knot end positions are calculated, and the dead knot border is set to the point where the knot reaches its maximum diameter. Finally, a parameterized knot model is created using regression models for the size and position of each knot.

The parameters used in the algorithm were originally set to achieve a high detection rate and low amount of false detections in Scots pine (*Pinus sylvestris* L.) and Norway spruce (*Picea abies* L. Karst) logs. In this study, we used the same parameters as in the Johansson et al. (2013) study, where further details can be found. For instance, we used a 15 mm mean value filter in the radial direction of CT stacks, the size of the median filter used in each CS was 510 × 510 mm, and so on. The exception was that the original algorithm employed a proportional shrinkage of 20 % the knots to account for diameter overestimation, this was changed to 10 % in this study since it resulted in a better predicted knot diameter.

Reference measurements of knots

Reference measurements were made manually in the CT images to enable validation of knot geometry including size, position, and end point. The measurements were done by drawing ellipses around knots in log CS's in the same manner as in Johansson et al. (2013). Ellipses for each non-occluded knot were drawn at radii at 10%, 20%, ..., 90% of the log radius. This yielded a total of nine ellipses per knot from the pith to the outer surface of the log. For occluded knots, ellipses were drawn to the knot end point, the position of which was marked in order to validate detection of the knot end. Overall, 57 knots were measured in this way, 23 in the white spruce log, 12 in Douglas-fir 1, 11 in western redcedar, and 11 in the Douglas-fir 2 log. All visible knots were measured, but in some cases it was not possible to tell if a small high

density object was a knot or something else, due to the low resolution. These objects were not measured, to avoid the risk of measuring an object that is not a knot.

Since the manual measurements were made in coarse resolution CT images and not on actual wood surfaces, there is a measurement error present. This error is even higher in the sapwood region, since the contrast between knot and regular wood density is lower than in the heartwood. For comparison, the manually drawn ellipses were parameterized using the same model as the automatically measured knots.

RESULTS AND DISCUSSION

Overall, 67 % of the manually marked knots were found by the algorithm. There is however a large spread as can be seen in Figure 2. The knot diameter detection accuracy was a bit worse than in Johansson et al. (2013), especially in terms of the mean error. This measure was negative overall, indicating that the algorithm underestimated the knot diameter. However, if the proportional shrinking of the knots were to be removed, the western redcedar log would have a large positive error instead, so on this limited data the current setup is a reasonable compromise, see also Figure 3a. The standard deviation and the RMSE of the knot diameter measurements were slightly worse than in Johansson et al. (2013). The differences between the logs could be due to the different species, but this material is much too limited to conclude anything in that direction. If more data were available, separate parameter setups for different species could be used, if any such differences were to be observed.

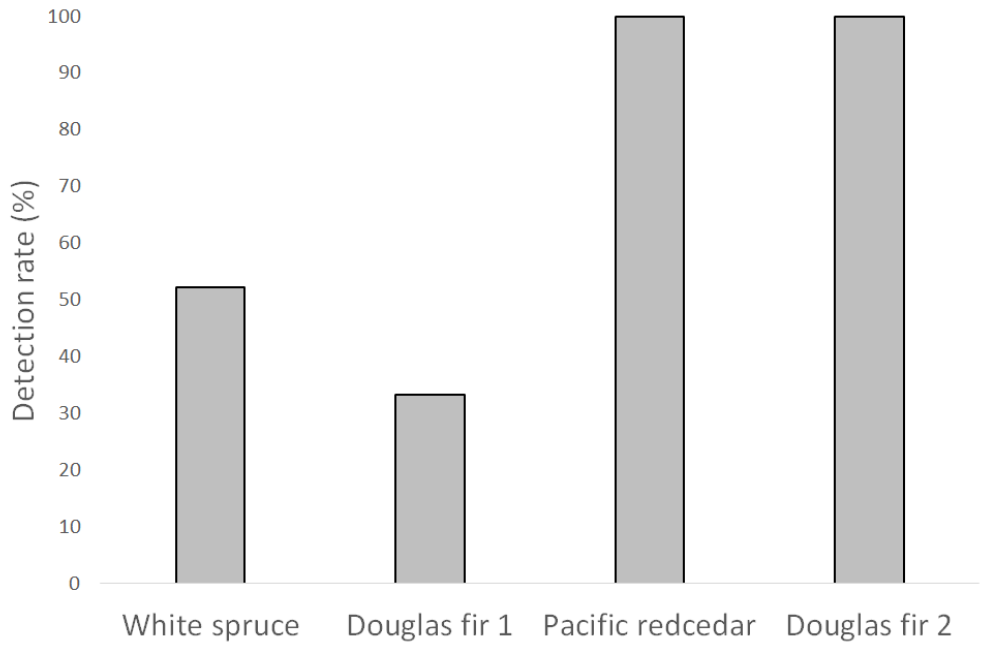

Figure 2: Knot detection rate for the four logs.

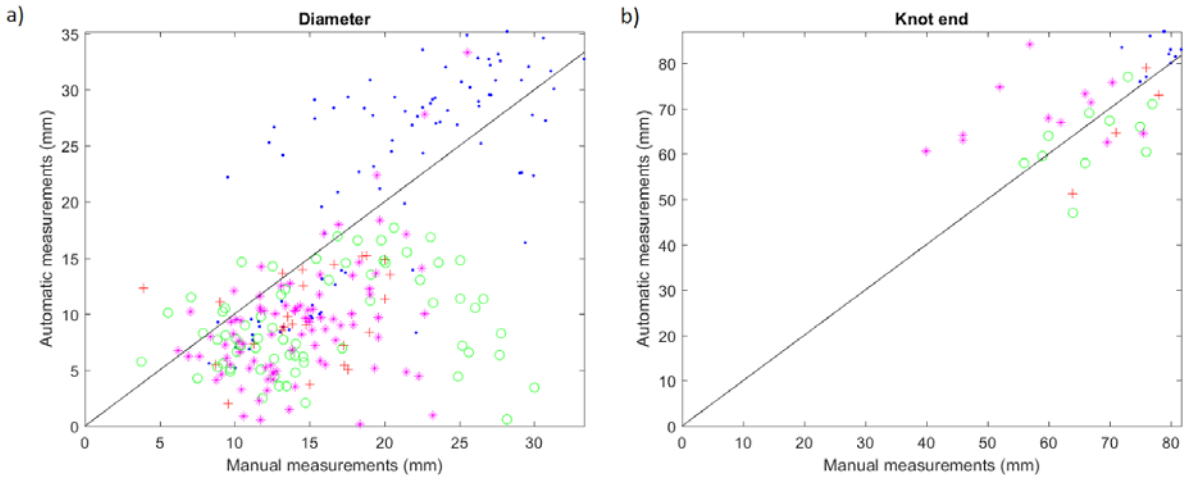

Figure 3: Automatic and manual measurements of knot diameter (a), and knot end position (b). Each point in (a) corresponds to one measurement of a knot in a concentric surface, while each point in (b) corresponds to one single knot. Magenta stars = white spruce, red plus signs = Douglas-fir 1, blue points = western redcedar, and green circles = Douglas-fir 2.

The detection accuracy of knot diameter, position, and end point is presented in Table 2. A negative mean error means that the algorithm underestimates the knot feature, and vice versa.

The height position detection accuracy was slightly better than Johansson et al. (2013), with a notable exception in the Douglas-fir 1 log, which was the log with the fewest measurements. The improved performance could be due to the higher longitudinal resolution (4 mm per slice) in the data used here, compared to Johansson et al. (10 mm per slice). For rotational position, the results of this study was slightly worse than in Johansson et al. (2013), again with an exception for the Douglas-fir 1 log where the performance was much worse than for the other logs.

In the case of rotational position, and knot diameter, the coarser cross-section resolution of our data compared to Johansson et al. (2013) could be the reason for the reduced performance.

For the knot end, the algorithm performed better on the material of this study than in Johansson et al. (2013) (Figure 3b). However, the number of observations are too small to draw any definite conclusions. In addition, our logs were of a rather small diameter which means that the knot end error in millimeters will be smaller even if the relative error is the same. In Johansson et al. (2013), the log top diameter ranged up to 332 mm compared to our maximum of 150 mm.

Table 2: Detection accuracy of knot diameter, position and end point for all logs. Diameter, height and rotational position sample size is measurements in concentric surfaces, while the knot end is measured per knot. R^2 values for knot position were omitted because they had meaningless statistical interpretation.

Log	Knot feature	Mean error	SD[a]	RMSE[b]	$R^{2,c}$	Sample size
white spruce	Diameter (mm)	-4.6	6.4	7.8	0.47	92
	Height position (mm)	-2.5	6.2	6.7	-	91
	Rotational position (°)	-1.6	5.6	5.8	-	91
	Knot end[d] (mm)	9.8	12	15	0.057	23
Douglas-fir 1	Diameter (mm)	-4.8	4.8	6.7	0.082	24
	Height position (mm)	9.3	10	14	-	22
	Rotational position (°)	-9.5	14	16	-	22
	Knot end (mm)	-5.3	6.5	7.7	0.89	12
western redcedar	Diameter (mm)	1.9	6.1	6.4	0.55	88
	Height position (mm)	0.18	7.7	7.7	-	88
	Rotational position (°)	-0.10	3.1	3.0	-	88
	Knot end (mm)	4.2	4.2	5.8	0.044	11
Douglas-fir 2	Diameter (mm)	-6.6	6.9	9.5	0.054	68
	Height position (mm)	-1.3	4.3	4.5	-	62
	Rotational position (°)	-0.39	5.3	5.2	-	62
	Knot end (mm)	-4.1	7.6	8.3	0.27	11
All	Diameter (mm)	-3.0	7.2	7.8	0.45	272
	Height position (mm)	-0.32	7.5	7.5	-	263
	Rotational position (°)	-1.5	6.5	6.6	-	263
	Knot end (mm)	2.6	10	10	0.29	57

[a] Standard deviation of detection error; [b] Root Mean Square Error; [c] Coefficient of determination; [d] Radial distance from pith to knot end, i.e. a straight line.

The data used in this study consist of only four logs, which means that the results presented are merely indicative. What can be seen in the results we do have, is that the detection rate is worse in data set 1 than in data set 2, but the difference in resolution is not very large so that is not a plausible explanation for the detection rate difference.

The low detection rate in the Douglas-fir 1 log could be explained by the fact that the knots in this log were gathered in one large group in the middle of the log. This might make distinction between different knots difficult for the automatic algorithm, and since the log was short and had few knots overall, only a handful of missed knots decreases the detection rate dramatically.

The low detection rate in the white spruce log was mainly due to the small internodal knots,

which are difficult to detect due to their small size and the low resolution of the X-ray images (Figure 4).

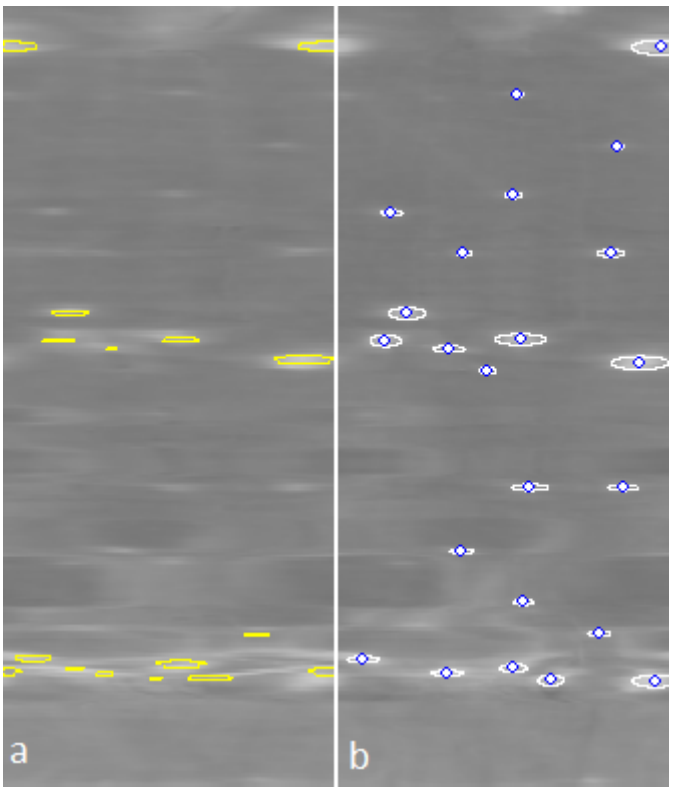

Figure 4: Detected and measured knots in a heartwood concentric surface of the white spruce log where a) shows knots detected by the automatic algorithm, and b) shows the knots measured manually. Horizontal axis is angular position and vertical axis is lengthwise position. Note that there is a slight difference between the two surfaces, since a) was calculated at a fixed distance from the pith in mm, while b) was calculated at a certain percentage of the detected outer shape. They are however located at the same approximate radius.

CONCLUSIONS

It can be concluded that for this limited amount of data from a coarse resolution CT scanner, it was possible to find the knots' position in the logs, however the knot size was not very well detected compared to Johansson et al. (2013). Small knots were difficult to find due to the coarse image resolution. Future work involves scanning more logs to get more data. If images of varying resolution could be tested, it could be possible to find the resolution needed for accurate knot detection both in terms of knot position and size.

ACKNOWLEDGEMENTS

The authors want to thank FPInnovations for providing the X-ray data for the study, especially Bruce Lehmann, Yuntao An and Edward Angus.

REFERENCES

An, Y. and Schajer, G. (2014a). Coarse-resolution cone-beam scanning of logs using Eulerian CT reconstruction. Part II: Hardware design and demonstration. In Residual Stress, Thermomechanics & Infrared Imaging, Hybrid Techniques and Inverse Problems, Volume 8 (pp. 21-29). Springer International Publishing.

An, Y. and Schajer, G. (2014b). Coarse-resolution cone-beam scanning of logs using Eulerian CT reconstruction. Part I: Discretization and algorithm. In Residual Stress, Thermomechanics & Infrared Imaging, Hybrid Techniques and Inverse Problems, Volume 8 (pp. 9-19). Springer International Publishing.

Baumgartner, R., Brüchert, F. and Sauter, U. (2010). Knots in CT scans of Scots pine logs. In The Future of Quality Control for Wood & Wood Products, The Final Conference of COST Action E53, Edinburgh, United Kingdom, 4-7 May 2010. Edited by Dan Ridley-Ellis and John Moore. pp. 343-351.

Guidiceandrea, F., Ursella, E. and Vicario, E. (2011). A high speed CT scanner for the sawmill industry. In Proceedings of the 17th International Nondestructive Testing and Evaluation of Wood Symposium, Sopron, Hungary, 14-16 September 2011. Edited by Ferenc Divos.

Johansson, E., Johansson, D., Skog, J. and Fredriksson, M. (2013). Automated knot detection for high speed computed tomography on *Pinus sylvestris* L. and *Picea abies* (L.) Karst. using ellipse fitting in concentric surfaces. *Computers and Electronics in Agriculture*, 96, pp. 238-245.

Longuetaud, F., Leban, J., Mothe, F., Kerrien, E. and Berger, M. (2004). Automatic detection of pith on CT images of spruce logs. *Computers and Electronics in Agriculture*, 44(2), pp. 107-119.

Longuetaud, F., Mothe, F. and Leban, J. (2007). Automatic detection of the heartwood/sapwood boundary within Norway spruce (*Picea abies* (L.) Karst.) logs by means of CT images. *Computers and Electronics in Agriculture*, 58(2), pp. 100-111.

Pietikäinen, M. (1996). Detection of knots in logs using x-ray imaging. PhD. VTT Technical Research Centre of Finland, Oulu, Finland.

Tong, Q., Duchesne, I., Belley, D., Beaudoin, M. and Swift, E. (2013). Characterization of knots in plantation white spruce. *Wood and Fiber Science*, 45(1), pp. 84-97.